

Exsolution in Clinoamphiboles

Abstract. Ten amphibole specimens from a variety of metamorphic rocks such as talc schists, eclogites, and metamorphosed iron formations contain lamellae of a second amphibole oriented parallel to $(\bar{1}01)$ or (100) , or both, of the host. Tremolites, actinolites, and hornblendes commonly have lamellae of a calcium-poor clinoamphibole with $P2_1/m$ space-group symmetry, or lamellae of cummingtonite with $C2/m$ space-group symmetry. Likewise cummingtonites and $P2_1/m$ clinoamphiboles commonly contain lamellae of calcium-rich $C2/m$ amphiboles such as tremolite. Results of x-ray diffraction, electron-probe, and microscope studies indicate that most lamellae result from unmixing of a homogeneous amphibole. The $P2_1/m$ clinoamphibole is analogous to the clinopyroxene pigeonite in agreement with the results of M. G. Bown.

Many have reported $(\bar{1}01)$ "parting" and (100) and $(\bar{1}01)$ twinning (I) in clinoamphiboles; there are fewer reports of exsolution (2-4). We now report on the compositions and crystallography of ten amphibole specimens containing intergrowths having second amphibole phases.

The talc-amphibole schists of the metamorphosed Grenville rocks, Gouverneur mining district, New York, contain ubiquitous tremolite showing very fine lamellae of a second amphibole oriented parallel to $(\bar{1}01)$ of the tremolite host (5). Single-crystal x-ray precession photographs of the tremolite from these two specimens (G-16 and G-24) show a strong diffraction pattern of the host tremolite and a second, weaker pattern of the thin lamellae. The unit-cell parameters (Table 1) of the host phase are typical of tremolite; the unit-cell parameters of the guest phase are similar to those expected from a typical cummingtonite, except that the space-group symmetry is $P2_1/m$ (or $P2_1$)—not $C2/m$ as found in all cummingtonites yet studied.

In typical tremolite crystals containing exsolution lamellae (Fig. 1) the lamellae oriented parallel to $(\bar{1}01)$ of the tremolite host are approximately 1μ wide. An electron-microprobe scan for Mn and Ca along the prism axis of a grain similar to those shown (Fig. 1) shows that there is a high concentration of manganese and a low concentration of calcium within the lamellae (Fig.

2A). Just the opposite effect was noted in the host tremolite. When the tremolite grains from specimen G-24 were excited by the unfocused electron beam in the electron probe, the tremolite host luminesced golden yellow; the included lamellae, dark red.

In some other primary grains of sample G-24, the host amphibole luminesces dark red and the included lamellae luminesce golden yellow. Probe scans along such grains give patterns (Fig. 2B) reciprocal to that shown in Fig. 2A, in that the lamellae are rich in calcium and the host is rich in manganese. Partial quantitative analysis with the probe indicates the composition



for the yellow-luminescing host phase, and



for the dark-red-luminescing host phase. The narrowness of the yellow- and red-luminescing lamellae prevents quantitative estimation of their chemical composition, but it seems probable that the yellow host and the yellow lamellae may have similar compositions, as well as the red host and the red lamellae.

It is clear that the schist from the area of the Wight mine contains two different primary clinoamphibole phases: tremolite and a manganese-rich clinoamphibole with $P2_1/m$ space-group symmetry. As the rock cooled (6), the $P2_1/m$ amphibole exsolved from the tremolite grains, and tremolite exsolved from the $P2_1/m$ amphibole grains.

Amphibole specimens from the International Talc mine No. 3, Talcville, New York, also were examined. The specimens (U.S. National Museum Nos. 115046 and 115545) were collected by Segeler (7), who described them as manganese-rich amphiboles closely related to cummingtonite. Partial quantitative microprobe analysis gives the following composition for the red-luminescing host areas in sample 115046:



A small amount of aluminum may substitute for silicon. X-ray precession photographs of several of the grains from specimen 115046 show the weaker diffraction pattern, of the tremolite lamellae, superimposed on a strong pattern of the $P2_1/m$ host amphibole (8) (Table 1).

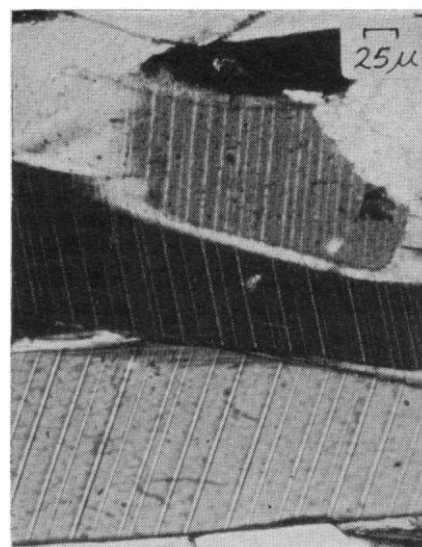


Fig. 1. Typical large tremolite grains (sample G-24) containing $(\bar{1}01)$ exsolution lamellae of the manganese-rich calcium-poor $P2_1/m$ clinoamphibole.

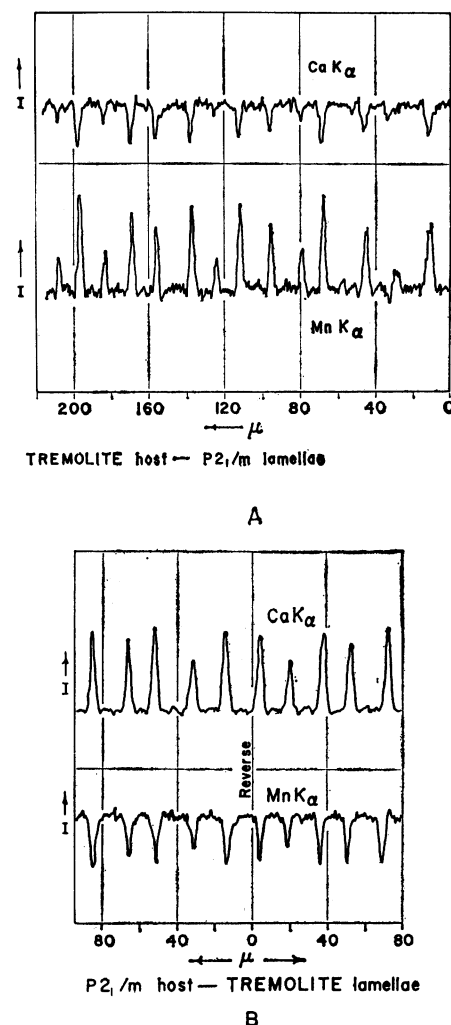


Fig. 2. Electron-microprobe scans for calcium and manganese in (A) a tremolite grain (sample G-24), showing exsolution lamellae of a $P2_1/m$ clinoamphibole, and (B) a $P2_1/m$ clinoamphibole grain (sample G-24), showing exsolution lamellae of tremolite.

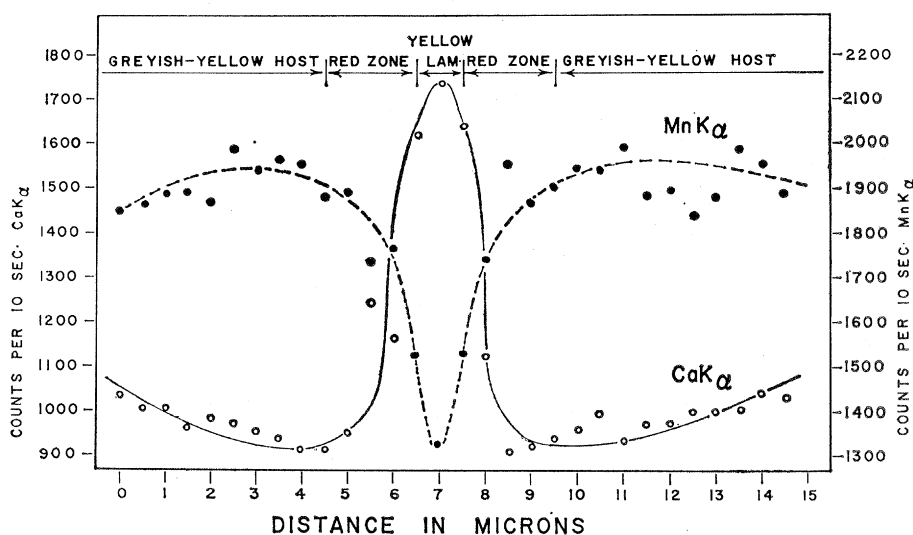


Fig. 3. Electron-microprobe scan for calcium and manganese across adjoining areas, luminescing grayish yellow, dark red, and golden yellow, in a grain from sample 115545. Note the calcium-depletion and manganese-enrichment zones at the shoulders of the central calcium peak.

Table 1. Unit-cell data for monoclinic amphiboles containing lamellar intergrowths of second clin amphiboles. Orientation relative to the host phase. Specimens are identified in italics.

Specimen	Orientation	Angstroms			β	Symmetry
		<i>a</i>	<i>b</i>	<i>c</i>		
<i>G-24, New York</i>						
Tremolite host		9.812	18.077	5.273	104°43'	<i>C</i> ₂ / <i>m</i>
<i>P</i> _{2₁/m lamellae}	($\bar{1}01$)	9.50	18.04	5.28	102°25'	<i>P</i> _{2₁/m}
<i>G-16, Arnold pit</i>						
Tremolite host		9.82	18.04	5.28	104°35'	<i>C</i> ₂ / <i>m</i>
<i>P</i> _{2₁/m lamellae}	($\bar{1}01$)	9.48	18.03	5.29	101°55'	<i>P</i> _{2₁/m}
<i>Bown (4), Wight mine</i>						
Tremolite host		9.81	17.95	5.27	104°45'	<i>C</i> ₂ / <i>m</i>
<i>P</i> _{2₁/m lamellae}	($\bar{1}01$)	9.51	17.95	5.27	102°0'	<i>P</i> _{2₁/m}
<i>115046, Talcville</i>						
<i>P</i> _{2₁/m host}		9.550	18.007	5.298	102°39'	<i>P</i> _{2₁/m}
Tremolite lamellae	($\bar{1}01$)	9.78	17.99	5.27	104°25'	<i>C</i> ₂ / <i>m</i>
<i>115545, Talcville</i>						
<i>P</i> _{2₁/m host}		9.50	17.99	5.30	102°40'	<i>P</i> _{2₁/m}
Tremolite lamellae	($\bar{1}01$)	9.80	17.99	5.28	104°40'	<i>C</i> ₂ / <i>m</i>
<i>HJ 163-60, Montana</i>						
Actinolite host		9.81	18.07	5.29	104°25'	<i>C</i> ₂ / <i>m</i>
<i>P</i> _{2₁/m lamellae}	($\bar{1}01$), (100)	9.48	18.07	5.30	102°5'	<i>P</i> _{2₁/m}
<i>HJ 182-60, Montana</i>						
Actinolite host		9.82	18.10	5.29	104°35'	<i>C</i> ₂ / <i>m</i>
Cummingtonite lamellae	($\bar{1}01$), (100)	9.48	18.10	5.30	102°10'	<i>C</i> ₂ / <i>m</i>
<i>MI2026, Minnesota</i>						
Cummingtonite host		9.55	18.28	5.32	102°10'	<i>C</i> ₂ / <i>m</i>
Hornblende lamellae	($\bar{1}01$), (100)	9.85	18.14	5.32	105°0'	<i>C</i> ₂ / <i>m</i>
<i>13, Labrador</i>						
Riebeckite-tr. host		9.77	18.04	5.29	104°20'	<i>C</i> ₂ / <i>m</i>
<i>P</i> _{2₁/m lamellae}	($\bar{1}01$)	9.48	18.04	5.30	102°15'	<i>P</i> _{2₁/m}
<i>1725, Norway</i>						
Hornblende host		9.85	18.01	5.29	104°45'	<i>C</i> ₂ / <i>m</i>
<i>P</i> _{2₁/m lamellae}	(100)	9.50	18.01	5.29	102°0'	<i>P</i> _{2₁/m}
Cummingtonite lamellae	($\bar{1}01$), (100)	9.49	18.01	5.29	101°55'	<i>C</i> ₂ / <i>m</i>
<i>138A, New Hampshire</i>						
Hornblende host		9.80	18.08	5.31	104°45'	<i>C</i> ₂ / <i>m</i>
Cummingtonite lamellae	(100), ($\bar{1}01$)	9.52	18.08	5.31	102°10'	<i>C</i> ₂ / <i>m</i>
Cummingtonite host		9.49	18.13	5.30	102°5'	<i>C</i> ₂ / <i>m</i>
Hornblende lamellae	(100), ($\bar{1}01$)	9.80	18.13	5.30	104°45'	<i>C</i> ₂ / <i>m</i>

Sample 115545 is unusual in containing amphibole grains in which the host luminesces grayish yellow; included lamellae luminescing golden yellow, approximately 1 μ thick, are oriented parallel to ($\bar{1}01$) of the host. The lamellae are usually bordered by wider (2 to 4 μ) zones that luminesce dark red. X-ray photographs of several grains show a strong diffraction pattern of a *P*_{2₁/m host and a weaker pattern of tremolite (Table 1).}

An electron-microprobe step scan for calcium and manganese across adjoining areas, luminescing grayish yellow, dark red, and golden yellow, of a single grain appears in Fig. 3; the lamellae luminescing golden yellow have a tremolitic composition, whereas the areas luminescing dark red and grayish yellow are calcium-poor and manganese-rich.

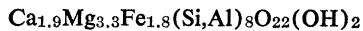
Electron-microprobe counting statistics (9) strongly indicate that the areas bordering the yellow lamellae are slightly enriched in manganese and slightly deficient in calcium relative to the host areas luminescing grayish yellow (Fig. 3). Partial microprobe analysis indicates that the composition of the host area is



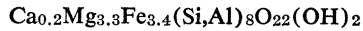
Small amounts of Na and Al may substitute for Ca and Si, respectively. The apparent chemical differences between the three types of areas—grayish-yellow host, golden-yellow lamellae, and bordering dark-red zones—are interpreted as being due to diffusion, calcium ions moving toward and manganese ions moving away from the golden-yellow area, with the result that dark-red zones immediately adjacent to the yellow lamellae are depleted in Ca and enriched in Mn relative to the grayish-yellow host.

Relations similar to those described have been found in amphiboles from various other metamorphic rocks. Quartz-amphibole-magnetite rocks (Nos. HJ 163-60 and 182-60) from a Precambrian iron formation, Ruby Mountains, southwest Montana (10), contain very complex amphibole intergrowths. In sample HJ 163-60, most amphibole grains have thick (5 to 50 μ), nearly colorless lamellae, of space-group symmetry *P*_{2₁/m, oriented parallel to ($\bar{1}01$) of pleochroic green actinolite. The two amphiboles are present in nearly equal amounts. In many crystals, colorless and green lamellae also are oriented parallel to (100), a plane common to both phases. Microprobe chemical anal-}

yses give the following approximate formula:

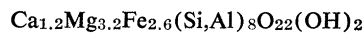


for the actinolite and

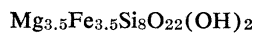


for the $P2_1/m$ amphibole. Sample HJ 182-60 contains amphibole intergrowths similar in appearance to those in sample HJ 163-60.

Single-crystal x-ray data (Table 1) and probe analysis show, however, that the pleochroic green actinolite lamellae are associated with colorless lamellae identified as cummingtonite, both phases having $C2/m$ space-group symmetry. The approximate formula for the actinolite is



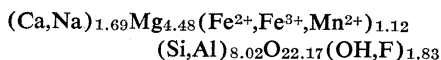
for the cummingtonite,



Because of the complex nature of the lamellar intergrowths, it is difficult to obtain accurate compositions. The mechanism of exsolution in the Ruby Mountains samples appears to be complicated and may be a two-stage process, formation of the $(\bar{1}01)$ lamellae preceding formation of the (100) lamellae. In some grains, the lamellae have coalesced to form homogeneous patches of a single amphibole.

Exsolution of hornblende on both $(\bar{1}01)$ and (100) of a cummingtonite host was found in a specimen (No. M12026) from a metamorphosed iron formation, Dunka River, Minnesota. The composition of the cummingtonite obtained by Bonnicksen (11) with the microprobe is $\text{Mg}_{2.31}\text{Fe}_{4.69}\text{Si}_8\text{O}_{22}(\text{OH})_2$. The hornblende lamellae are less than 1μ thick and make up only a small part of the grain.

A (riebeckite-tremolite) host amphibole, with lamellae of a $P2_1/m$ clin amphibole oriented parallel to $(\bar{1}01)$, was found in a metamorphosed specularite - (aegirine - augite) - (riebeckite - tremolite)-calcite-quartz rock (No. 13) from the Wabush Iron Formation, southwest Labrador (12). The grains appear very similar to those of sample G-24 (Fig. 1). Klein (12) gives the chemical composition of the bulk amphibole sample as



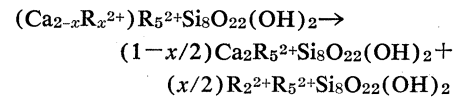
Hornblendes from an eclogite (No. 1725) of the Eiksundsdaal Eclogite Complex, Hareidlan, Sunnmøre, Norway (13), were found to be intergrown with

two types of amphiboles. In one grain the host hornblende was intergrown parallel to (100) with a $P2_1/m$ clin amphibole. Single-crystal x-ray data (Table 1) indicate that this grain comprises about 60 percent hornblende and 40 percent $P2_1/m$ amphibole. It is not apparent whether or not exsolution has occurred; the (100) intergrowth may be primary or may be due to a partial inversion or alteration from a high-temperature form. X-ray examination (Table 1) of a second grain from this sample showed that very fine (100) and $(\bar{1}01)$ lamellae of cummingtonite are included within the hornblende host; the cummingtonite composes about 10 percent of the grain and appears to have formed by exsolution.

Lastly we report (Table 1) the unit-cell data for the individual phases of submicroscopic cummingtonite-hornblende intergrowths found in a garnet-quartz-amphibole-apatite rock (I38A) from Richmond, New Hampshire (14). The composition may vary continuously from nearly 100 percent hornblende to 100 percent cummingtonite across a single grain. In addition to the submicroscopic intergrowth of hornblende and cummingtonite on (100), very fine visible lamellae of cummingtonite in hornblende and of hornblende in cummingtonite, each oriented parallel to $(\bar{1}01)$ of its host, are present in many grains.

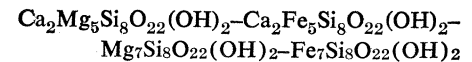
These observations indicate that amphiboles of the tremolite-ferroactinolite series, and also certain hornblendes (3), often have chemical compositions such that the large M4 cation positions are

not fully occupied by calcium and sodium. Some of the smaller metal atoms, such as Fe, Mn, and Mg, must enter the M4 position. This atomic configuration is stable at high temperature but becomes unstable at lower temperatures, and a phase rich in Mn, Fe, or Mg exsolves. An idealized reaction (one assuming complete unmixing) is written

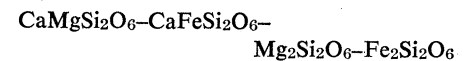


Conversely, cummingtonite-grunerite amphiboles or $P2_1/m$ -type amphiboles slightly enriched in calcium may exsolve a calcium-rich amphibole such as tremolite or actinolite, geologic conditions permitting. In fact the exsolution is not complete, and the host and exsolved phases still contain some Ca or R^{2+} component.

The amphibole-crystal chemical relations in the system



appear to resemble remarkably the pyroxene relations (15) in the system



Schematic representations of the compositional range of pyroxene and amphibole types of structure, based on the literature and our observations, appear in Fig. 4, A and B, respectively. A solid-solution series between tremolite and ferroactinolite is represented at the top of Fig. 4B.

All calcium-rich amphiboles so far examined are monoclinic and have $C2/m$ space-group symmetry. The calcium-poor amphiboles (Fig. 4B, bottom) include: (i) anthophyllite, which is orthorhombic and has $Pnma$ space-group symmetry; (ii) cummingtonite, which is monoclinic and has $C2/m$ space-group symmetry; and (iii) the monoclinic amphibole possessing $P2_1/m$ space-group symmetry.

Our studies revealed no amphiboles with $(\bar{1}01)$ "parting" or twinning (1, 4); twinning on (100), however, is common. An attempt was made to homogenize samples G-24 and 115545 in a run of 66-day duration at 800°C and 1000 bars of water pressure; single-crystal x-ray photographs showed no change in the relative intensities of the diffraction patterns of tremolite and the $P2_1/m$ clin amphibole, so that homogenization was undetectable. Although electron-microprobe, textural, and x-ray evidence, and the analogy to the pyroxene

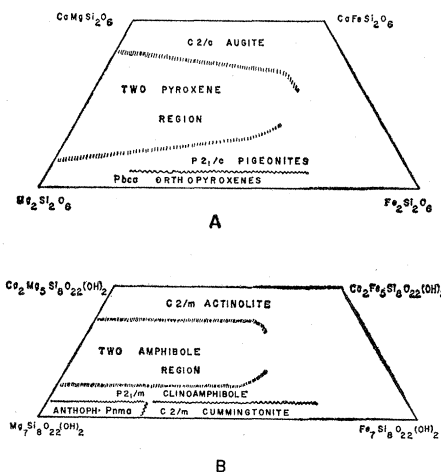


Fig. 4. Schematic representation of the composition range of (A) pyroxenes in the system $\text{CaMgSi}_2\text{O}_6 - \text{CaFeSi}_2\text{O}_6 - \text{Mg}_2\text{Si}_2\text{O}_6 - \text{Fe}_2\text{Si}_2\text{O}_6$, and (B) the amphiboles in the system $\text{Ca}_2\text{Mg}_5\text{Si}_8\text{O}_{22}(\text{OH})_2 - \text{Ca}_2\text{Fe}_5\text{Si}_8\text{O}_{22}(\text{OH})_2 - \text{Mg}_7\text{Si}_8\text{O}_{22}(\text{OH})_2 - \text{Fe}_7\text{Si}_8\text{O}_{22}(\text{OH})_2$.

phase relations, strongly suggest that the (101) lamellae are due to exsolution, other modes of origin of these lamellae are possible.

Published chemical analyses and recent electron-probe analyses indicate that the anthophyllite and cumingtonite crystal structures contain very little calcium—probably less than 2 percent CaO by weight. We expect, however, that the $P2_1/m$ clin amphiboles, which are analogous to the pigeonite clinopyroxenes, are richer in calcium.

MALCOLM ROSS
J. J. PAPIKE

U.S. Geological Survey,
Washington, D.C. 20242

PAUL W. WEIBLEN
Department of Geology and Geophysics,
University of Minnesota, Minneapolis

References and Notes

1. The indices (100) and (101) refer to the C-centered clin amphibole setting. In the I-centered setting, which is often used in the earlier literature, the (101) plane becomes (001).
2. B. Askund, *Arsbok* 17(6) (1923); —, W. L. Brown, J. V. Smith, *Amer. Mineralogist* 47, 160 (1962); E. Callegari, *Classe Sci. Mat. Nat.* 78, 273 (1965–66).
3. R. A. Binns, *Mineral. Mag.* 35, 306 (1965).
4. M. G. Bown, *Amer. Mineralogist* 51, 259 (abstr.) (1966). Bown's unit-cell data for tremolite and $P2_1/m$ "clin anthophyllite" were transformed from an I-centered cell to a C-centered unit cell which conforms to the standard setting.
5. M. Ross, W. L. Smith, W. H. Ashton, *Amer. Mineralogist*, in press.
6. A. E. J. Engel and C. G. Engel [*Bull. Geol. Soc. Amer.* 71, 1 (1960)] estimate that the temperatures of formation of the Grenville gneiss assemblages that enclose the talc-tremolite schists of the Gouverneur mining district were about 500° to 600°C.
7. C. G. Segeler, *Amer. Mineralogist* 46, 637 (1961).
8. Bown (4) has suggested the name clin anthophyllite for a $P2_1/m$ clin amphibole from the Wight mine, New York; Segeler (7) referred to the manganese-rich amphiboles from Talville, N.Y. (Nos. 115046 and 115545), as tirodite. Until the composition limits of this amphibole structure type are better understood, we suggest that it be termed $P2_1/m$ clin amphibole.
9. The error in total counts is expected to be less than 3 percent two-thirds of the time; within 6 percent 95 percent of the time.
10. These rocks are being studied by H. L. James and K. W. Shaw, U.S. Geological Survey; we thank them for letting us examine these specimens and for advice on the petrogenesis. Also we thank others (11–14) for generously furnishing the necessary amphibole specimens.
11. B. Bonnicksen, University of Minnesota, personal communication. E. C. Perry, Jr., and B. Bonnicksen [*Science* 153, 528 (1966)] estimate the maximum temperature of these rocks at about 700°C, on the basis of O^{18}/O^{16} fractionation between coexisting magnetite and quartz.
12. C. Klein, Jr., *J. Petrol.* 7, 246 (1966).
13. H. H. Schmitt, thesis, Harvard University, 1964.
14. Now being studied by P. Robinson, H. W. Jaffe (University of Massachusetts), and C. Klen, Jr. (Harvard University).
15. A. Poldervaart and H. H. Hess, *J. Geol.* 59, 472 (1951); G. M. Brown, *Mineral. Mag.* 31, 511 (1957); M. G. Bown and P. Gay, *ibid.* 32, 379 (1960).
16. Studies of silicate minerals (11); publication authorized by the director, U.S. Geological Survey.

12 December 1967

Carcinogens 3,4-Benzpyrene and 3-Methylcholanthrene: Induction of Mitochondrial Oxidative Enzymes

Abstract. Sections of liver from rats injected with 3,4-benzpyrene and 3-methylcholanthrene, when incubated in mediums specific for the histochemical demonstration of mitochondrial oxidative enzymes, show greater activity of several of these enzymes than do sections from control rats. This observation was confirmed by comparison of the staining of mitochondria isolated from the control and from "induced" rats. The fact that an inhibitor of protein synthesis, actinomycin D, effectively diminished the stimulation provided evidence that the stimulation of activity is due to an increase in enzyme synthesis, generally called induction.

Adaptive changes whereby pharmacologically active substances stimulate metabolic activity, by enhancing the physiological synthesis of additional amounts of enzymes, may alter the duration and intensity of drug action in animals and man (1). Acceleration of the metabolism of various lipid-soluble drugs by liver microsomal enzymes responsible for inactivation reactions has been demonstrated (1). Thyroid hormone has been shown biochemically (2) to stimulate the activity of several rat-liver microsomal enzymes, as well as to enhance incorporation of amino acid into protein by liver microsomes. Phenobarbital, 3,4-benzpyrene, and 3-methylcholanthrene also have been shown (3) to enhance markedly this latter function of the microsomal liver fraction. Adaptive stimulation of mitochondrial oxidative enzymes by thyroxine has also been demonstrated (4) biochemically in investigations of the mechanism of control of basal metabolic rate by thyroid hormone. Further similarity between the different types of inducing agents is indicated by a report (5) of the probable enhancement of mitochondrial oxidative enzymes in livers of rats treated with phenobarbital. Such similarity is not unexpected, since concomitantly with enhancement of either the microsomal or the mitochondrial oxidative enzymes there occurs proliferation of the protein of these organelles; although the microsome is primarily responsible for protein synthesis within the cell, the mitochondrion has its own capability (6) for production of protein enzymes.

We tried to demonstrate the enhancement, in tissue sections, of mitochondrial oxidative enzymes with chromogenic histochemical methods specific for these enzymes. Use of an appropriate substrate and the ditetrazolium salt nitro blue tetrazolium (nitro-BT) (7) permits deposition of diformazan pigment at the intramitochondrial sites of dehydrogenase activity (8). Another

reagent, 3,3'-diaminobenzidine, which undergoes oxidative polymerization, accurately delineates the localization of cytochrome *c* of the cytochrome oxidase triplet to mitochondria in heart, liver, and kidney (9).

We confirmed histochemically an increase in mitochondrial α -glycerophosphate dehydrogenase, malic dehydrogenase, succinic dehydrogenase, dihydronicotinamide adenine dinucleotide (DPNH) diaphorase, and cytochrome oxidase in tissue sections of livers of rats made hyperthyroid. We also confirmed histochemically the earlier observation (5), on isolated mitochondria, of the enhancement of mitochondrial malate dehydrogenase and succinic dehydrogenase in livers of rats injected with phenobarbital; the livers of these rats also showed an increase in cytochrome oxidase activity.

The differences in absorbance of the histochemical pigments observed in control and in experimental tissue sections were reproducible. Moreover, the histochemical methods used permitted direct observation of the particular organelles involved in the reaction. Classical biochemical methods such as measurement of oxygen utilization (10) require prior isolation of the organelles under study by differential centrifugation (11) of tissue homogenate. We then applied our methods to study of liver sections of rats given the doses of 3,4-benzpyrene and 3-methylcholanthrene that had been used to "induce" microsomal enzymes (1). A definite increase was observed although the profile of increased mitochondrial dehydrogenase activity differed from that obtained by stimulation with thyroid hormone or phenobarbital.

Table 1 summarizes the histochemical observations on rat livers for several dehydrogenases and cytochrome oxidase after stimulation by triiodothyronine (T_3), phenobarbital, 3,4-benzpyrene, and 3-methylcholanthrene; we have graded the intensities of staining,